

## SUPPLEMENTAL MATERIAL

### UNC119 is required for G protein trafficking in sensory neurons

Houbin Zhang, Ryan N. Constantine, Sergey Vorobiev, Yang Chen, Jayaraman Seetharaman, Yuanpeng Janet Huang, Rong Xiao, Gaetano T. Montelione, Cecilia D. Gerstner, M. Wayne Davis, George Inana, Frank G. Whitby, Erik M. Jorgensen, Christopher P. Hill, Liang Tong, and Wolfgang Baehr

#### Inventory

##### Supplemental Table 1

UNC119 Crystallographic Data and Refinement Statistics

##### Supplemental Table 2

Comparison of the RMSD values for each of the six UNC119 chains and their associated ligands.

#### Supplemental Figures

##### Figure S1 Comparison of UNC119, PrBP/ $\delta$ , and RhoGDI structures

Fig. S1A. Greek key motif of the  $\beta$ -sandwich fold common to the three structures

Fig. S1B. Ribbon representation of the geranylgeranyl binding protein RhoGDI (1DOA) and the prenyl binding protein PrBP/ $\delta$  (1KSH)

Fig. S1C. Sequence alignment of human UNC119, PrBP/ $\delta$ , and RhoGDI

##### Fig. S2 Structural alignment of UNC119 with PrBP/ $\delta$ and RhoGDI

Fig. SA,B. Structural alignment of UNC119 with PrBP/ $\delta$  and RhoGDI

Fig. S2C. Electron density surrounding the lauroyl-T $\alpha$  peptide

##### Fig. S3. Overlap of the UNC119 carbon- $\alpha$ coordinates and associated ligands

##### Fig. S4 A–J. ODR-3 and GPA-13 trafficking defects in mutant *C. elegans* olfactory neurons

**Table S1: UNC119 crystallographic data and refinement statistics**

Data		
Crystal	HR3066a <sup>a</sup>	Au10pe
Space Group	P2 <sub>1</sub> 2 <sub>1</sub> 2 <sub>1</sub>	P2 <sub>1</sub> 2 <sub>1</sub> 2 <sub>1</sub>
Unit Cell Dimensions	a=77.89, b= 79.56, c=189.72	a=78.55, b=79.71 , c=189.59
Resolution (Å)	50.0 – 1.95	30.0 – 2.00
Resolution (Å) (high-resolution shell)	(2.02 – 1.95)	(2.07 – 2.00)
# Reflections measured	1,169,802	1,252,665
# Unique reflections	166,290 <sup>a</sup>	82,342
Redundancy	7.0	15.2
Completeness (%)	99.6 (100)	100 (100)
<I/σ(I)>	26 (2.9)	11 (2.5)
Mosaicity (°)	0.37	1.1
Rsym <sup>b</sup>	0.088 (0.537)	0.116 (0.701)
Refinement		
Resolution (Å)	40.51 – 1.95	29.37 – 1.99
Resolution (Å) – (high-resolution shell)	(1.97 – 1.95)	(2.04 – 1.99)
# Reflections used for refinement	165,606 <sup>a</sup>	78,089
# Reflections in Rfree set (%)	8,332 (5.0)	4,139 (5.3)
R <sup>c</sup>	0.191 (0.247)	0.200 (0.226)
Rfree <sup>d</sup>	0.214 (0.251)	0.250 (0.276)
RMSD: bonds (Å) / angles (°)	0.005 / 1.3	0.012 / 1.304
<B> (Å <sup>2</sup> ): Tα peptide residues / # atoms	N/A	41 / 268
<B> (Å <sup>2</sup> ): UNC119 only / # atoms	33 / 8,265	29 / 8,299
<B> (Å <sup>2</sup> ): water molecules / # water	41 / 803	39 / 793
φ/ψ most favored (%)	99	97

Values in parenthesis refer to data in the high resolution shell.

<sup>a</sup> Friedel pairs were used in phasing and refining HR3066a.

<sup>b</sup> Rsym =  $\sum |I - \langle I \rangle| / \sum I$  where I is the intensity of an individual measurement and  $\langle I \rangle$  is the corresponding mean value.

<sup>c</sup> R =  $\sum ||F_o| - |F_c|| / \sum |F_o|$ , where |F<sub>o</sub>| is the observed and |F<sub>c</sub>| the calculated structure factor amplitude.

<sup>d</sup> Rfree is the same as R calculated with a randomly selected test set of 5% (HR3066a<sup>a</sup>) or 5.3% (Au10pe) reflections that were never used in refinement calculations.

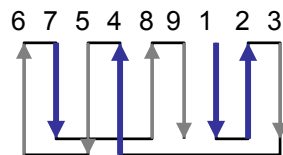
**Table S2. Comparison of the RMSD values for each of the six UNC119 chains and their associated ligands.**

Structures were overlapped on the UNC119 protein carbon- $\alpha$  atoms only. Ligand atoms were not included in the overlap calculation. RMSD values are given for the overlap of all protein atoms in each chain, all atoms related to residue 501 (glycine and the attached lauroyl group), and the carbon- $\alpha$  trace for the peptide attached to the lauroyl group in each ligand.

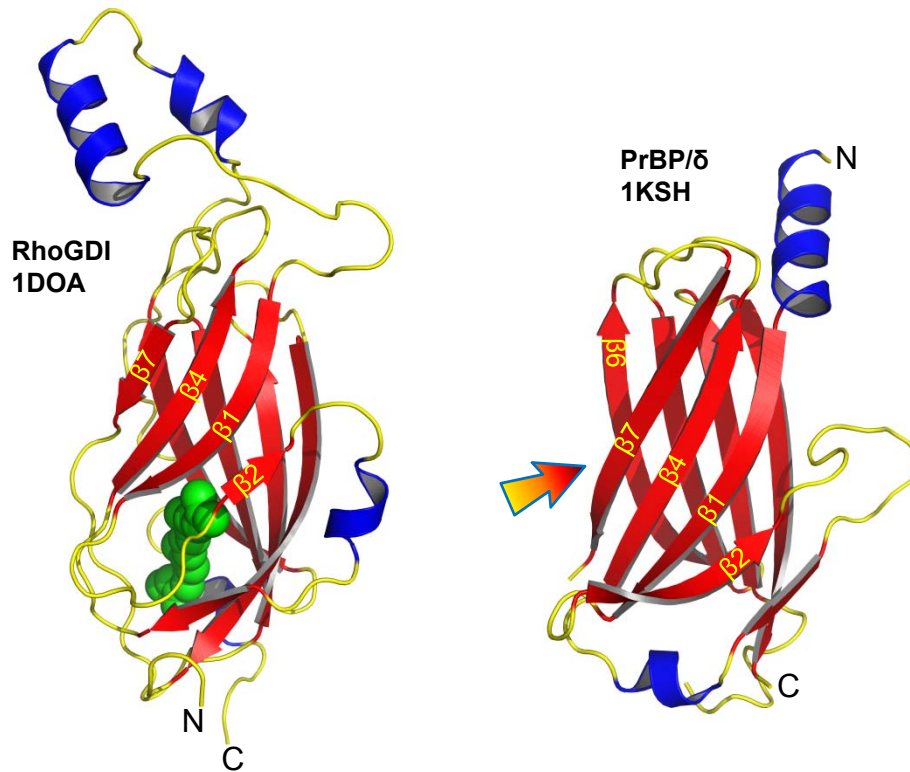
Chains Overlapped	RMSD for all protein atoms	RMSD for residue 501 <sup>a</sup>	RMSD of C $\alpha$ trace <sup>b</sup>
B on A	0.373	0.252	0.190 (501-507)
C on A	0.459	0.315	0.180 (501-504)
D on A	0.320	0.284	0.182 (501-504)
E on A	0.449	0.370	0.323 (501-503)
F on A	0.458	0.635	0.424 (501-507)

<sup>a</sup>RMSD values calculated using all atoms on residue 501 with residue 501 defined as glycine plus the attached lauroyl group.

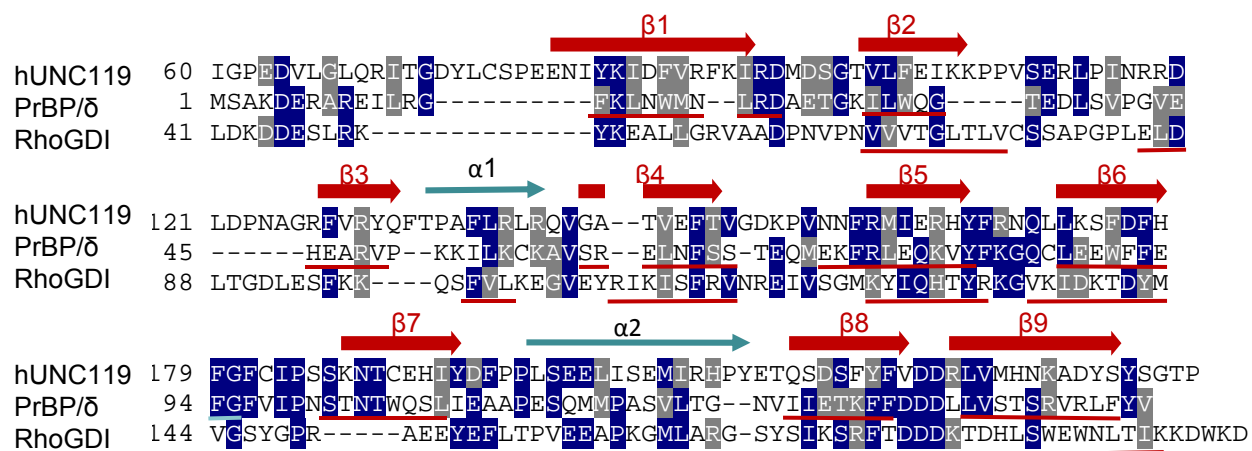
<sup>b</sup>Numbers in parentheses refer to residues on the ligand from which the RMSD values were calculated.



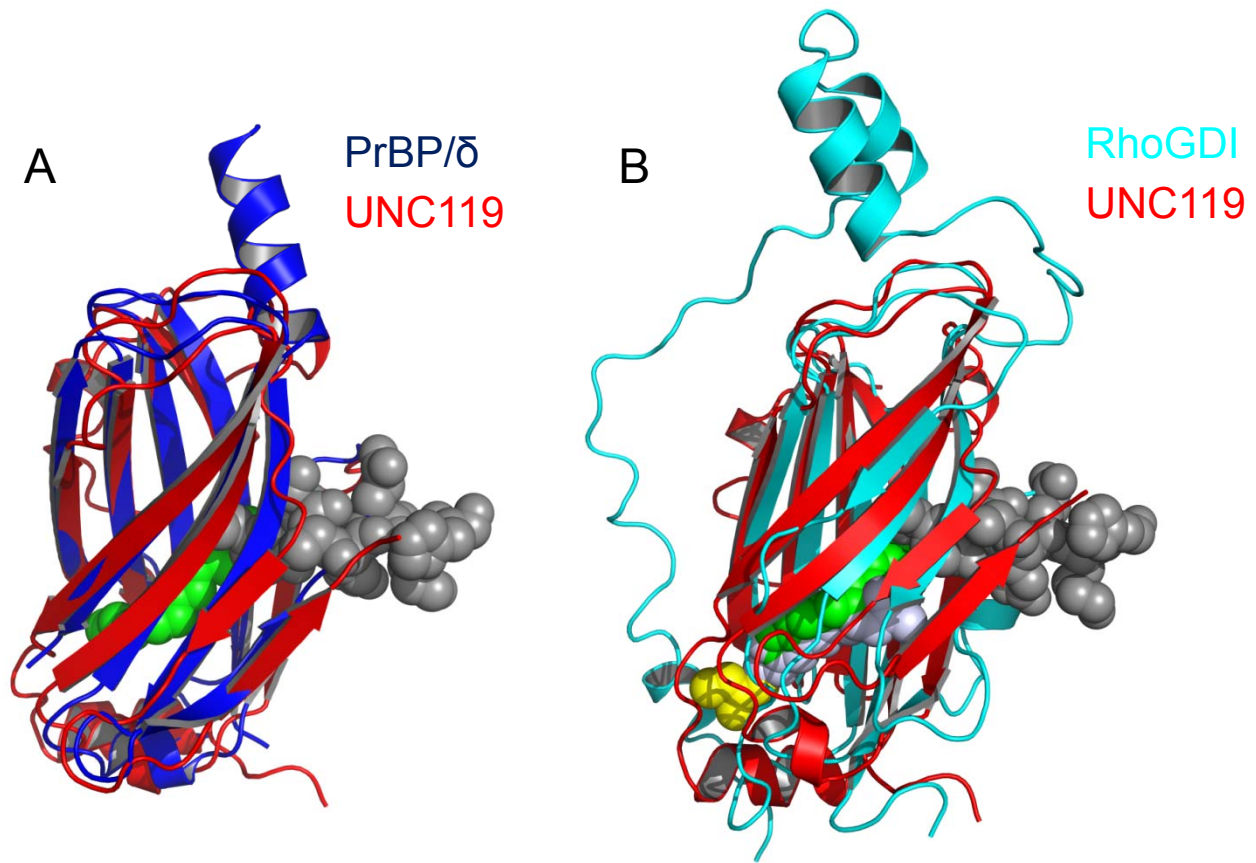
**Figure S1A** The Greek Key Motif in UNC119, RhoGDI and PrBP/ $\delta$  (related to Fig. 1). Greek key motif of the  $\beta$ -sandwich fold common to the three structures. Blue arrows depict the strands that form one  $\beta$ -sheet, while gray arrows depict strands of the second  $\beta$ -sheet.



**Figure S1B** Ribbon representation of the geranylgeranyl binding protein RhoGDI (1DOA) and the prenyl binding protein PrBP/ $\delta$  (1KSH). RhoGDI is shown with Cys-geranylgeranyl of CDC42 present in its binding pocket. The presumed entrance to the hydrophobic pocket of PrBP/ $\delta$  is indicated with an arrow. Note that entrances to the hydrophobic pocket in UNC119 (Fig. 4A,B) and RhoGDI are located at the opposite edge of the  $\beta$ -sandwich fold. Figure created with PyMOL ([www.pymol.org](http://www.pymol.org)).

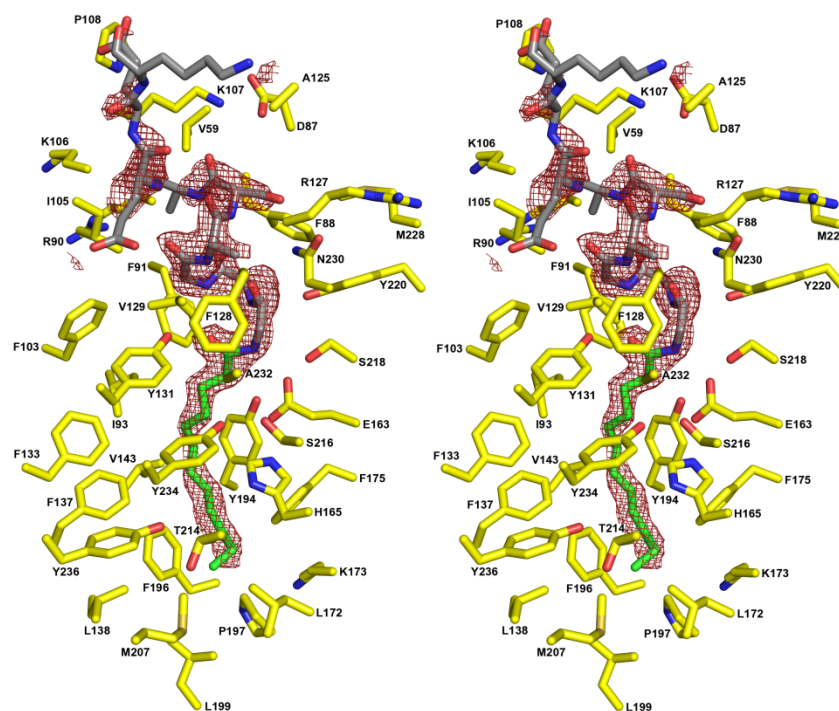


**Figure S1C** Sequence Alignment of Human UNC119, PrBP/δ, and RhoGDI. Only C-terminal residues of UNC119 (60-240) and RhoGDI (41-204) are shown. β-strands are depicted as large red arrows for UNC119 and are underlined in red for PrBP/δ and RhoGDI. Identical residues are highlighted blue and similar residues gray.



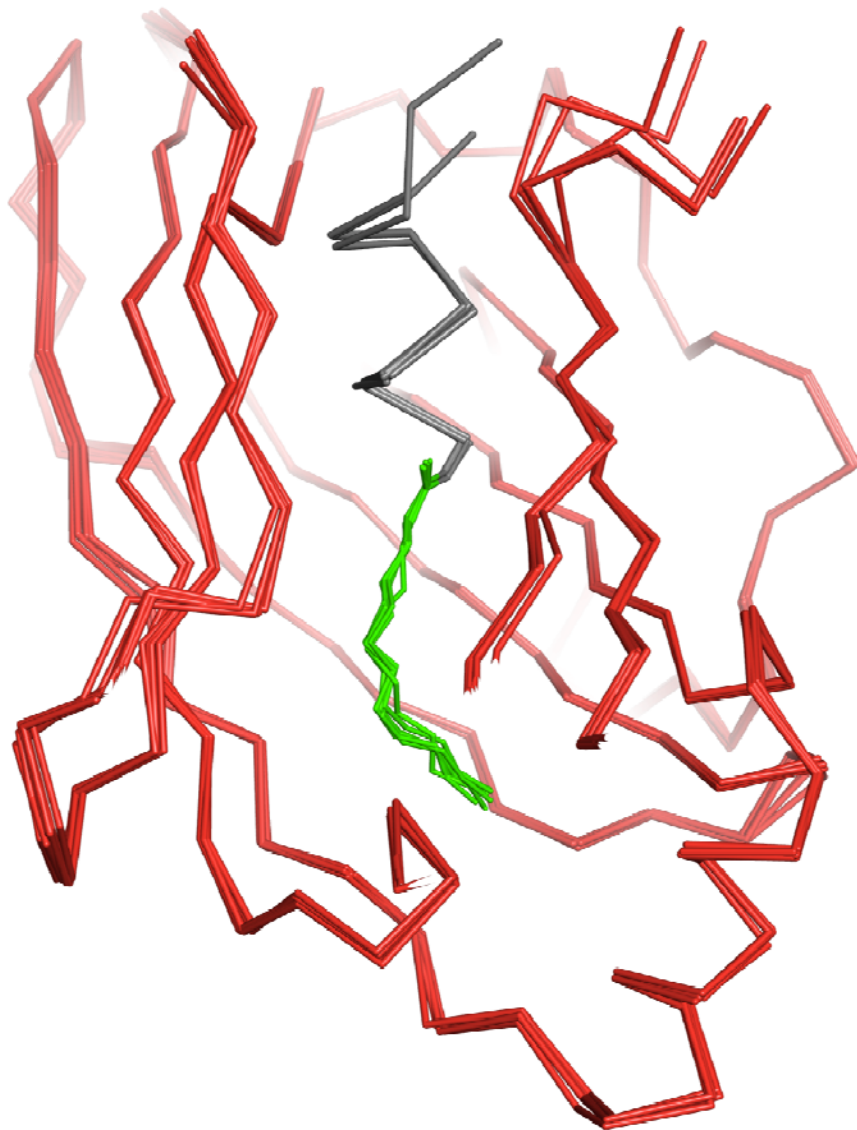
**Figure S2A,B** Structural Alignment of UNC119 with PrBP/δ and RhoGDI (related to Figure 4). **(A)** UNC119 (red) (PDB 3RBQ) aligned with PrBP/δ (blue). The T $\alpha$  peptide is shown in dark gray and the acyl chain in green. Figure created with PyMOL ([www.pymol.org](http://www.pymol.org)). **(B)** UNC119 (red) aligned with RhoGDI (cyan). The T $\alpha$  peptide is shown in dark gray and the acyl chain in green. The geranylgeranyl chain of the GTPase CDC42 bound to RhoGDI is shown in light gray. Figures created with PyMOL ([www.pymol.org](http://www.pymol.org)).

Fig. S2C  
Zhang et al.



**Figure S2C** Electron density surrounding the Lauroyl-T $\alpha$  peptide. A stereoview showing a simulated annealing Fo-Fc omit map contoured at 2.5 sigma (red mesh). Phases were calculated following deletion of the ligand, application of random shifts (0.1 Å), and refinement of the resulting model. UNC119 residues that comprise the walls of the cavity are shown with yellow carbon atoms, the acyl chain is colored green, and residues that comprise the remainder of the T $\alpha$  peptide are colored gray.





**Figure S3** Overlap of the UNC119 carbon- $\alpha$  coordinates and associated ligands. The UNC119 carbon- $\alpha$  coordinates for each of the six molecules in the asymmetric unit were overlapped and are shown in red. In each of the molecules the lauroyl-GAGASAEKHK ligand is bound in very similar fashion. The acyl group of the ligand is shown in green and the ordered peptide residues of the ligand are colored gray. Figure created with PyMOL ([www.pymol.org](http://www.pymol.org)).

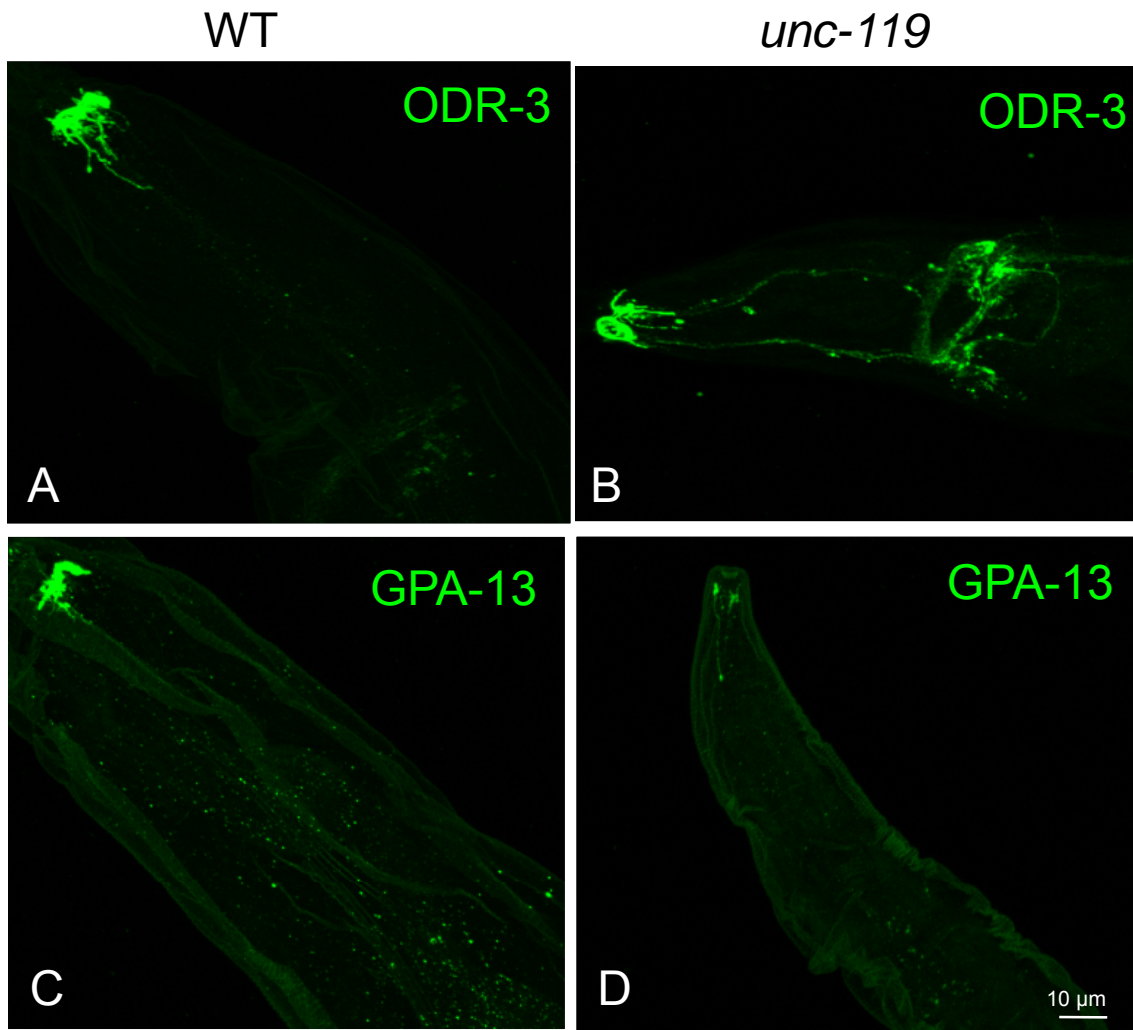


**Figure S4 A–D** ODR-3 and GPA-13 trafficking defects in mutant *C. elegans* olfactory neurons. (**A–D**), localization of ODR-3 (A, B) and GPA-13 (C,D) in wild-type (A,C) and *unc-119* mutant (B,D) *C. elegans* olfactory neurons. In wild-type neurons, ODR-3 and GPA-13 (green) traffic normally to the olfactory cilia. In mutant neurons, the G protein subunits are mislocalized (B, ODR-3) or exhibit decreased expression (D, GPA-13).

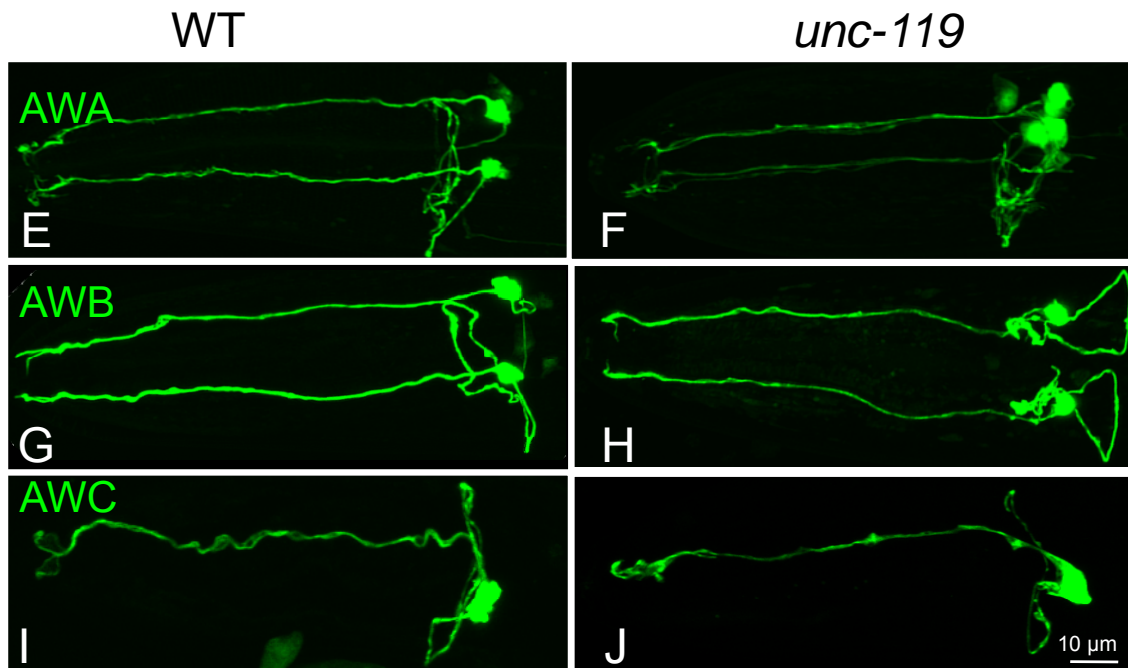


**Figure S4 E–J** ODR-3 and GPA-13 trafficking defects in mutant *C. elegans* olfactory neurons. **E–J**, structural integrity of AWA, AWB and AWC Cilia in *unc-119 C. elegans* and restoration of ODR-3 and GPA-13 Localization. GFP was specifically expressed in AWA neurons (E,F), AWB neurons (G,H), and AWC neurons (I,J) of wild-type (left column) and *unc-119* mutant (right column) *C. elegans* worms. Reporter constructs were *odr-10::gfp* for AWA, *str-1::GFP* for AWB, and *str-2::GFP* for AWC. The structural integrity of these neurons is not compromised in the mutant (F,H,J) when compared to WT (E,G,I). Please note that transgene *kyls140* in the *unc-119* mutant background only expressed GFP in one of the two AWC neurons (**Fig. S4I,J**), while some of the transgenic worms expressed GFP in both AWC neurons (unpublished data). Similar phenomena have been reported for other mutants (Troemel et al., *Cell* **99**, 387-398 (1999)).

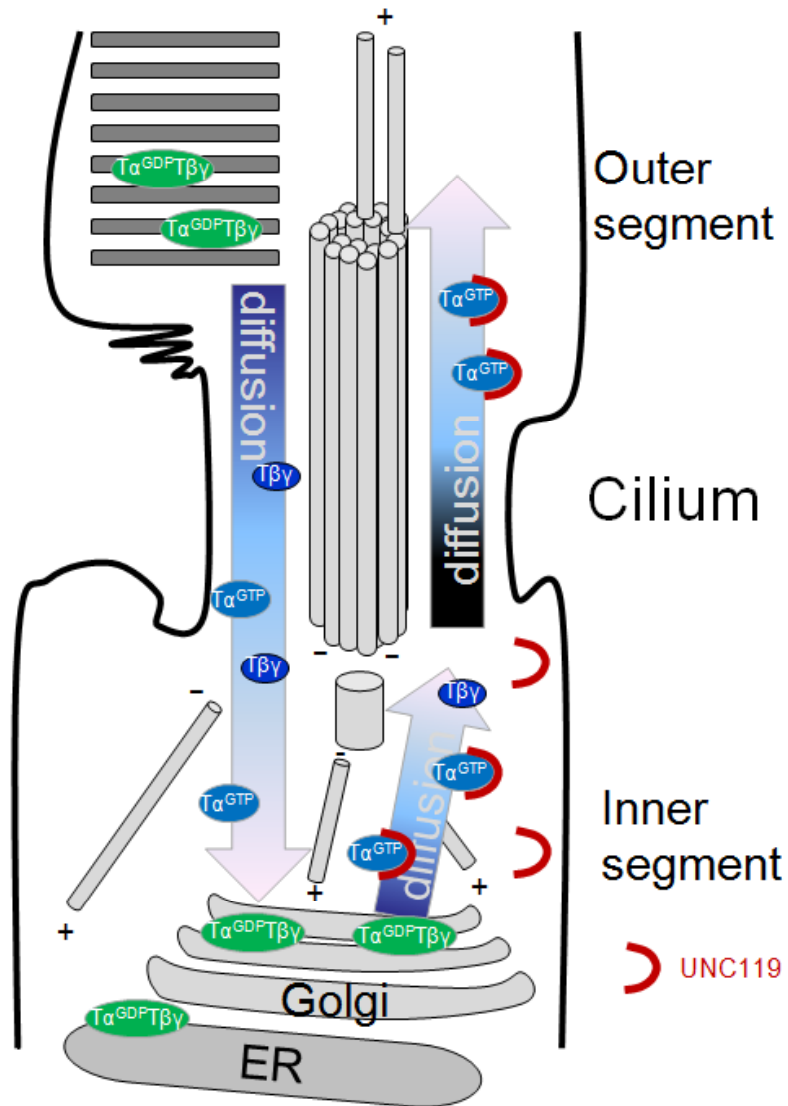


**Fig. S5** Light-induced translocation of transducin and return to the outer segment. **(A)** Schematic depiction of transducin translocation. Under intense light,  $T\alpha^{GTP}$  and  $T\beta\gamma$  translocate separately to the inner segment and following GTP hydrolysis, associate with inner segment membranes as a heterotrimer  $T\alpha^{GDP}\beta\gamma$ . Following GDP/GTP exchange, which is very slow in the absence of rhodopsin,  $T\alpha^{GTP}$  is eluted from the membrane by the acyl-binding protein UNC119.  $T\beta\gamma$  elutes and associates with a prenyl binding protein, either PrBP/ $\delta$  or phosducin<sup>37</sup>. Both  $T\alpha$ /UNC119 and  $T\beta\gamma$ /PrBP diffuse freely and re-associate with a destination membrane after GTP hydrolysis. The destination membrane could be the cell membrane at the distal inner segment where IFT cargo is assembled or one of many outer segment disks.

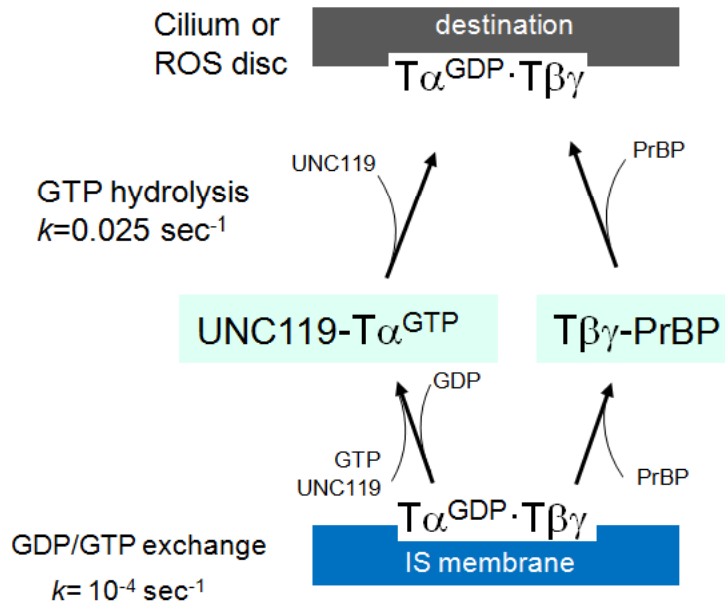


**Fig. S5** Light-induced translocation of transducin and return to the outer segment. **(B)** Kinetic analysis of return to the OS. In the absence of a GEF (rhodopsin), solubilization of  $T\alpha$  governed by GDP/GTP exchange is slow ( $k=10^{-4}/\text{sec}$ )<sup>38</sup>, and is most likely the rate limiting step for the return of transducin. Likewise, the hydrolysis of  $T\alpha^{GTP}$  is slow ( $k=0.025 \text{ sec}^{-1}$ ) in the absence of GAP, but not rate-limiting. GDP/GTP exchange maintains a rate constant of  $0.0001/\text{sec}$ , resulting in only 0.01% of  $T\alpha$  solubilized per second<sup>38</sup>, or one-third of  $T\alpha/\text{hour}$ , which explains the slow return to the outer segment.

## Reference List

1. Hanzal-Bayer,M., Renault,L., Roversi,P., Wittinghofer,A., & Hillig,R.C. The complex of Arl2-GTP and PDE delta: from structure to function. *EMBO J.* **21**, 2095-2106 (2002).
2. Troemel,E.R., Sagasti,A., & Bargmann,C.I. Lateral signaling mediated by axon contact and calcium entry regulates asymmetric odorant receptor expression in *C. elegans*. *Cell* **99**, 387-398 (1999).